Hindawi
Adsorption Science & Technology
Volume 2023, Article ID 6985657, 18 pages
https://doi.org/10.1155/2023/6985657

Research Article

Development of Durian Rind/Polypyrrole Composite and Its Application in Removing of Anionic Dyes

Yan Wang, Zijing Dai, Jiaqi Zha, and Wenqing Wei

College of Life and Health Sciences, Anhui Science and Technology University, Chuzhou, 233100 Anhui, China

Correspondence should be addressed to Yan Wang; yanwang0129@126.com

Received 19 May 2023; Revised 21 July 2023; Accepted 11 August 2023; Published 17 August 2023

Academic Editor: Adrián Bonilla-Petriciolet

In this study, polypyrrole (PPy) was introduced into durian rind (DR) by in situ polymerization method to prepare durian rind/polypyrrole (DR/PPy) composite. The resulting material was characterized using scanning electron microscope (SEM), transmission electron microscope (TEM), infrared spectroscopy (IRS), and X-ray diffraction (XRD). Then, the removing performance of the DR/PPy material for anionic dyes was explored. The impact of key variables such as the amount of adsorbent, initial dye concentration, pH, adsorption temperature, and contacting time on the adsorption efficiency was examined. The result disclosed that the adsorption efficiency of DR/PPy for methyl orange, sunset yellow, and amaranth was satisfactory. In pH of 7, initial concentration of 100 $\mu g\,mL^{-1}$, and DR/PPy dosage of 1.5 $g\,L^{-1}$, the removal efficiency reached 97.31%, 98.48%, and 98.20%, respectively. The adsorptive kinetics and thermodynamic process were analyzed subsequently. The adsorption of anionic dyes on DR/PPy conforms to the pseudo-second-order kinetic and Langmuir isotherm models with maximum adsorption capacity ($q_{m,max}$) of 193.05, 171.23, and 147.71 $mg\,g^{-1}$ for methyl orange, sunset yellow, and amaranth, respectively. Finally, a possible mechanism involved in the adsorption system was put forward. This study implies a reasonable feasibility for the effective utilization of waste to control the pollution.

1. Introduction

Currently, the emission of pollutants has increased dramatically due to the rapid urbanization and expanding scale of industrial production. Among these pollutants, colored dye wastewater produced by the textile industry has been deemed as the main contaminant related to its mutagenic and noxious properties. Meanwhile, the extremely high chroma of dyes can inhibit the photosynthesis of aquatic plants, which causes the disrupting of the ecological balance in water bodies [1, 2]. Therefore, it is particularly important to take appropriate methods to reduce or remove dyes before discharging into environment. At present, the techniques for the disposal of dye wastewater mainly include adsorption, chemical precipitation, photocatalytic degradation, and electrochemical degradation [3–6]. Generally speaking, each method owns its inherent advantages and disadvantages. Among these aforementioned methods, adsorption has always been mentioned as one of the most versatile, low-cost, environment-friendly, and efficient techniques for pollutant treatment. Normally, the performance of pollutant elimination is predominantly depended on the peculiarities of the adsorbent, including the specific surface area and degree of exposure of the functional groups. Therefore, numerous scholars will have to commit substantial effort to develop applicable and cost-effective adsorbents. Durian rind, as a kind of agricultural waste, is discarded in large quantities every year. In the interest of environment, the exploitation and utilization of durian rind is very important. Some authors have utilized durian rind, as a low-cost adsorbing material, to eliminate dyes and heavy metals from aqueous solution [7–10]. Asbollah et al. monitored the synergistic adsorption effect on the elimination of acid red-1 and methylene blue by durian rind [11]. These reports manifested that it is necessary to exploit the potential application of durian rind in the adsorption field.

Recently, the emerging of polymer-based adsorbents especially conductive polymer, which has obtained increasing attention owing to their satisfactory features such as good biocompatibility, excellent stability, simple synthesis

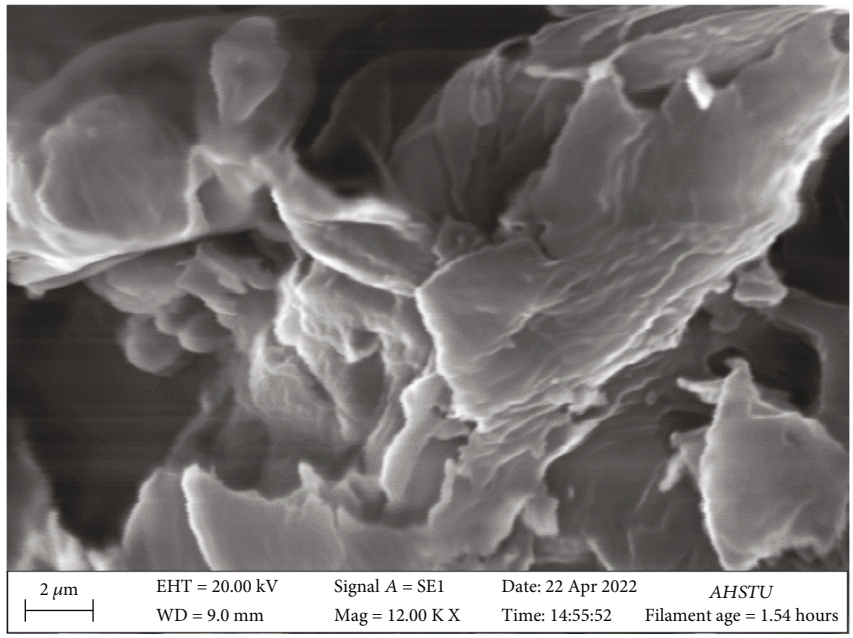

(a)

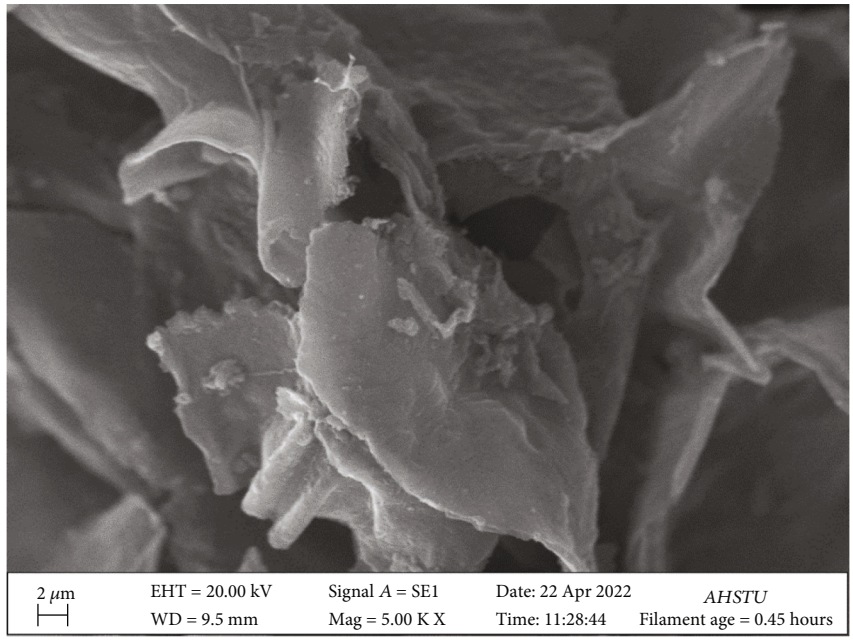

(b)

Figure 1: Continued.

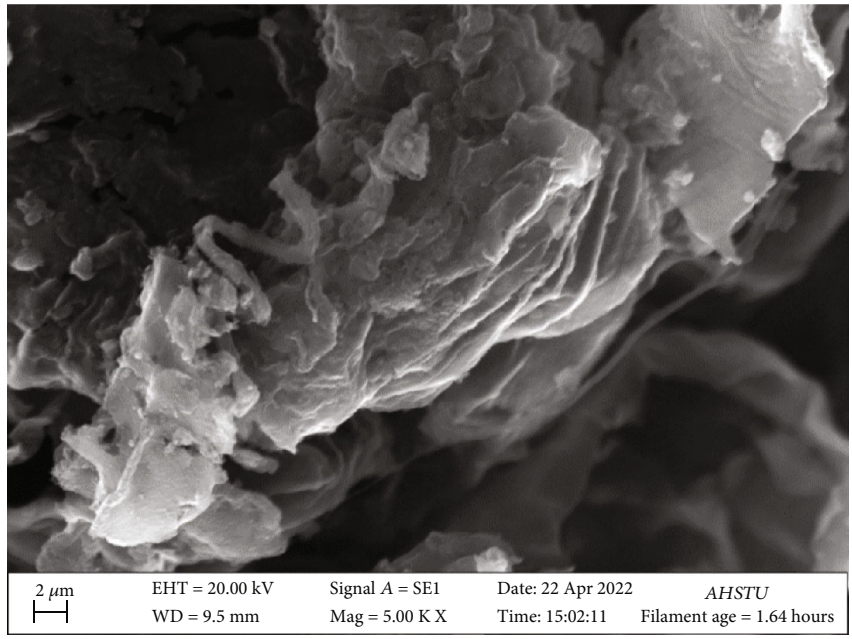

(c)

Figure 1: SEM image of (a) DR, (b) DR/PPy, and (c) amaranth-loaded DR/PPy.

process, nontoxicity, and low cost, has attracted extensive attention of scholars. Polypyrrole, as a heterocyclic conjugated conductive polymer, has been commonly used. PPy has a positive charge center in its structure, which can selectively remove anionic pollutants from aqueous solutions through electrostatic and π-π interactions. This behavior endows polypyrrole a unique application in the field of sewage disposal. Actually, the synthesized process of polypyrrole is relatively simple. However, the pure polypyrrole prepared by traditional methods is prone to aggregation and difficult to control pores, which becomes a limiting factor in adsorption field [12]. In order to improve its performance, scientists try to compound polypyrrole with other materials. Polypyrrole was deposited on the surface of nanocellulose via in situ oxidative polymerization method to prepare nanocellulose polypyrrole composite (NCPPY). The resulting composite exhibited a satisfactory efficiency for the simultaneous removal of chromium and Congo red [13]. Khadir et al. used sisal as a material to synthesize sisal/polypyrrole/polyaniline for RO5 elimination from aqueous media [14]. Therefore, a reasonable modification of biomass with PPy would be an ideal method to improve the property of biomass.

In view of the excellent prospects of polypyrrole in the field of adsorption and the urgent status of durian rind, this study is aimed at preparing durian rind/polypyrrole composite material as an adsorbent for wastewater pollutant treatment. In this work, polypyrrole was introduced into durian rind by in situ polymerization method to produce DR/PPy composite. The prepared DR/PPy material was analyzed via SEM, TEM, IRS, and XRD. Typical anionic dyes were selected to evaluate the adsorption performance. Experiments in batch were performed to explore the effect of DR/PPy dosage, initial concentration of dye, pH, adsorption temperature, and contacting time on the removal performance. The adsorptive kinetics, isotherm, and thermodynamics were specifically conducted and evaluated. Finally, a possible mechanism involved in the adsorption system was proposed. This research provides a reasonable idea and reference for the effective utilization of waste and the control of dye pollution.

2. Materials and Methods

2.1. Reagents and Materials. Pyrrole (99%), octylphenol ethoxylate 10 (OP-10, 98%), $FeCl_3$ (99%), methyl orange (98%), sunset yellow (85%), amaranth (85%), and other required reagents (AR) procured from Macklin, China, were used. Durian rind supplied by a local market, China, was used.

2.2. Preparation of DR/PPy Composite. The prepared method details were referred to our previous research [1]. Firstly, the durian rind with the outer shell removed was dried in a vacuum drying oven at 60°C for 48 h. The dried samples were crushed and sieved to get 20-40 mesh samples. Then, 1.0 g of DR powder was mixed with 25 mL of pyrrole aqueous solution (0.2 M) stirring at 250 rpm for 20 h. On the other hand, an appropriate amount of OP-10 (used as surfactant) was dispersed in 50 mL of distilled water and then added together with 2.0 g of $FeCl_3$ at 25°C in a magnetic stirring for 1 h. The mixture in the first container was again stirred for 5 h under ice bath condition by the dropwise addition of $FeCl_3$ solution. Then, the obtained product was separated and washed alternately with ethanol and distilled water to clear the impurities. The resulting DR/PPy composite was dried and used in the following experiments.

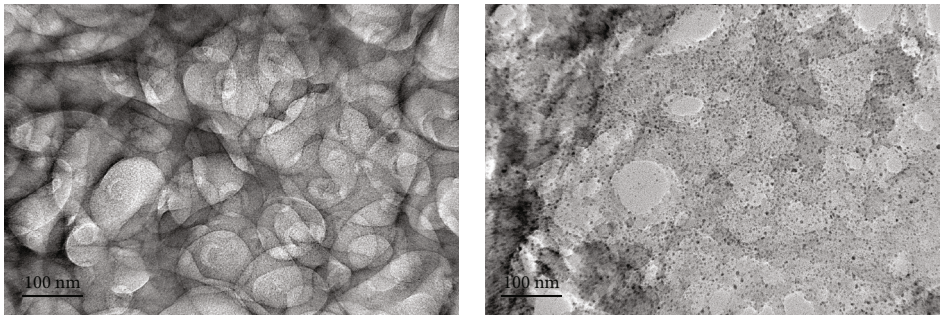

(a) (b)

Figure 2: TEM image of (a) DR and (b) DR/PPy.

2.3. Characterization of DR/PPy Composite. Herein, SEM, TEM, IRS, and XRD were requisitioned to characterize the structure and properties of the sample of DR/PPy composite. The image of surface of DR/PPy composite (coated with gold) was captured using EVO18 SEM (ZEISS, Germany). The TEM was performed on JEM-2100F instrument (JEOL, Japan) to determine the shape of DR/PPy material. IRS spectra were recorded with KBr pellets by FTIR-850 infrared spectroscopy (Gangdong, China) with a range of 4000-400 cm^{-1}. The XRD pattern was operated on a XD-3 diffractometer (Persee, China) in the region of 2θ from 5° to 90° at a scanning speed of 10° min^{-1}.

2.4. Dye Adsorption Procedure. The adsorption behavior of DR/PPy composite was evaluated for methyl orange, sunset yellow, and amaranth removal at various conditions. Batch experiments were conducted, and parameters including the amount of DR/PPy, initial dye concentration, pH, adsorption temperature, and contacting time were investigated in the research studies. All of the data were carried out three times, and the corresponding mean value was recorded in this work. Generally, 0.03 g of DR/PPy particle was mixed with 20 mL of dye solution (C_0 of 100 $\mu g\,mL^{-1}$, the pH was adjusted by 0.1 M HCl or 0.1 M NaOH before experiment) in conical flask. The mixture was shaken in an incubator shaker at 160 rpm for a specific time at a required temperature. Then, the DR/PPy material was separated from the system of dye solution by filter after the adsorption. The remaining dye of methyl orange, sunset yellow, and amaranth concentration in aqueous media was determined by UV/Vis spectrophotometer at the respective wavelength of 464 nm, 482 nm, and 521 nm, respectively. Variables of DR/PPy amount (0.01-0.08 g), initial dye concentration (50-300 $\mu g\,mL^{-1}$), pH (3-11), contacting time (5-360 min), and temperature (20-50°C) were considered in our experimental process. Equation (1) and equation (2) were adopted to calculate the removal efficiency (E) of these examined dyes and the adsorption capacity (q_e) of DR/PPy, respectively.

$$E(\%) = \frac{(C_0 - C_1) \times V}{C_0 \times V} \times 100\% = \frac{(C_0 - C_1)}{C_0} \times 100\%, \quad (1)$$

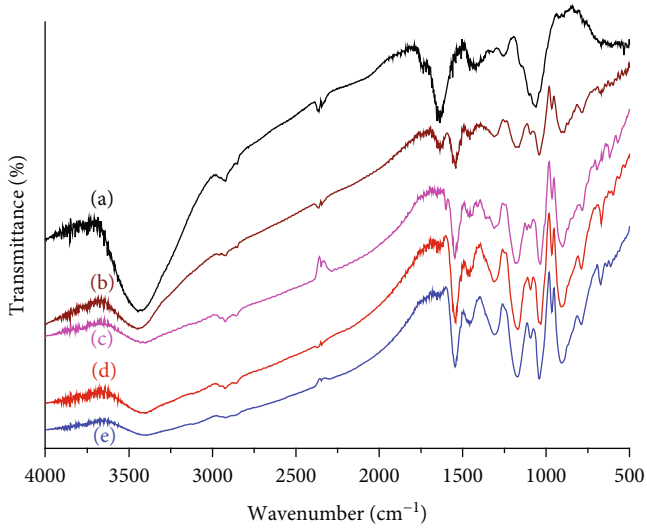

Figure 3: IRS spectra of (a) DR, (b) DR/PPy, (c) methyl orange-loaded DR/PPy, (d) sunset yellow-loaded DR/PPy, and (e) amaranth-loaded DR/PPy.

$$q_e = \frac{(C_0 - C_1) \times V}{m}, \quad (2)$$

where V (mL) represents the volume of dye solution, m (g) corresponds to the weight of the adsorbent, C_0 ($\mu g\,mL^{-1}$) represents the initial concentration of dye, and C_1 ($\mu g\,mL^{-1}$) displays the concentration of dye at any time.

Pseudo-first-order, pseudo-second-order, and intraparticle diffusion kinetic equations as well as the Freundlich and Langmuir isotherm models (equations (3), (4), (5), (6), and (7), respectively) were employed to assess the adsorption system.

$$\log (q_e - q_t) = \log q_e - \frac{k_1}{2.303} t, \quad (3)$$

$$\frac{t}{q_t} = \frac{1}{k_2 q_e^2} + \frac{1}{q_e} t, \quad (4)$$

$$q_t = k_p t^{1/2} + c, \quad (5)$$

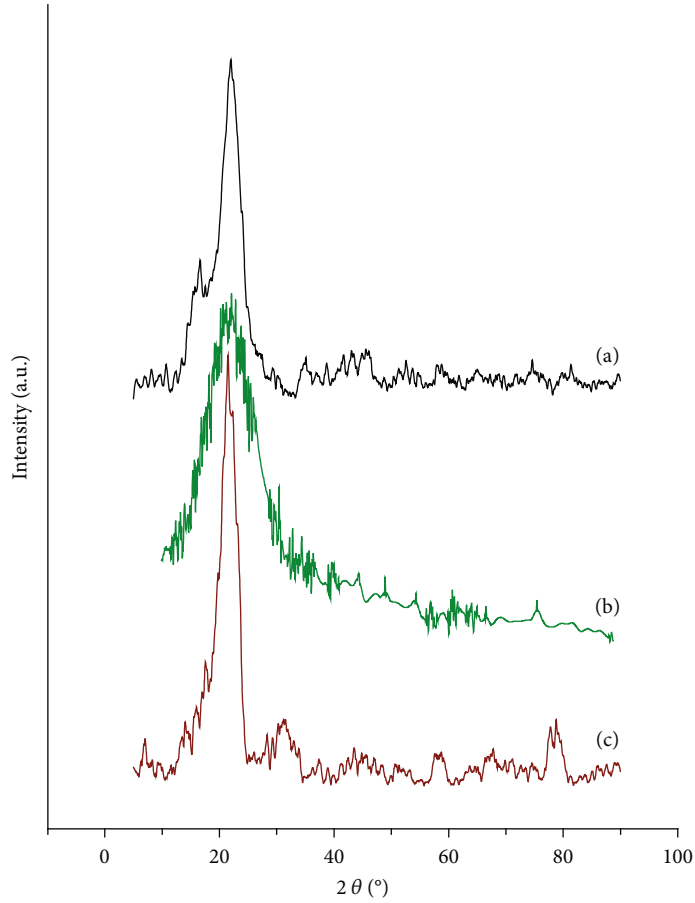

Figure 4: XRD patterns of (a) DR, (b) PPy, and (c) DR/PPy.

$$\ln q_e = \ln K_f + \frac{1}{n} \ln C_e, \tag{6}$$

$$\frac{C_e}{q_e} = \frac{1}{K_l q_m} + \frac{C_e}{q_m}, \tag{7}$$

where t (min) is the contacting time in adsorption; q_e (mg g^{-1}) and q_t (mg g^{-1}) represent the adsorption capacity at equilibration and at any given time, respectively; k_1 (min^{-1}), k_2 (g mg^{-1} min^{-1}), and k_p (mg g^{-1} min$^{-0.5}$) represent the rate constant of pseudo-first-order, pseudo-second-order, and diffusion models, respectively; c (mg g^{-1}) corresponds to the constant connected with the thickness of the boundary layer; K_f (L mg^{-1}) correspond to a Freundlich constant related to the adsorption capacity of the adsorbent; n is a parameter connected with the adsorption intensity; C_e (μg mL^{-1}) is the equilibrium concentration of dye in aqueous media; K_l (L mg^{-1}) displays a Langmuir constant reflecting the adsorption energy; and q_m (mg g^{-1}) represents the maximum adsorption capacity.

3. Results and Discussion

3.1. Characterization of Materials. The surface morphological structure of DR, DR/PPy, and dye-loaded DR/PPy (taking the removal of amaranth as an example, i.e., amaranth-loaded DR/PPy) is intuitively presented in Figure 1. The surface of DR was relatively smooth with a lamellar shape at the edge of the fold (Figure 1(a)). However, after modification with PPy, rough surface could be found in the DR/PPy as compared to the durian rind. It is clear that some aggregations of spherical particles were appeared on its surface (Figure 1(b)). It could be attributed to the coating cover of PPy particles on the surface of durian rind during the preparation of DR/PPy. This structure was also observed by Khadir et al. after modification of sisal with polypyrrole and polyaniline [14]. The relative morphology of DR/PPy was slightly changed after adsorption, which might be due to the cover of surface of DR/PPy via dye molecules (Figure 1(c)). Figure 2 exhibits the TEM images of DR and DR/PPy material. The result showed that there was changing in the morphology of DR after modification with PPy. Moreover, the dark spots of PPy nanoparticles with diffused form were dispersedly embedded in the matrix of DR. The comparison result indicated the successful introduction of PPy into DR material. Mashkoor and Nasar also discovered approximately similar structure for the chitosan/PPy/Fe_3O_4 in TEM image [12].

The IRS spectra of DR and DR/PPy illustrated in Figure 3 showed the appearance of new peaks in DR/PPy. The broad peak at 3440 cm^{-1} of DR/PPy was concerned in the O-H stretching vibration. The characteristic peaks at 1545 and 1461 cm^{-1} in DR/PPy are assigned to the C=C stretching vibration at pyrrole ring [1, 12]. This result

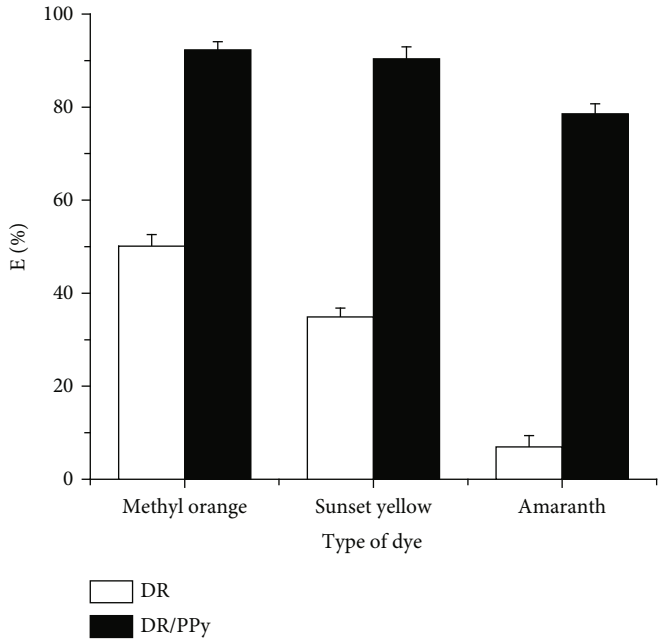

Figure 5: Comparison in the removal efficiency of DR and DR/PPy (conditions: DR/PPy dosage of 1.0 g L^{-1}, temperature of 20°C, contacting time of 23 h, pH of 7, and C_0 of 100 μg mL^{-1}).

indirectly indicates the successful introduce of PPy into DR. In addition, the stretching vibration peaks of C-C and C-N appear at 1460 and 1303 cm^{-1}, respectively. The peaks at 1308, 1175, 1040, 967, and 787 cm^{-1} correspond to the stretching vibration of C-N, C-H in-plane vibration, N-H in-plane vibration, C-H out-of-plane deformation, and C-H wagging vibration of pyrrole ring, respectively [12, 15]. The result clearly confirmed the successful introduction of PPy into DR. IRS spectra of DR/PPy after adsorption of methyl orange, sunset yellow, and amaranth are also illustrated in Figure 3. The peaks related to DR/PPy shifted to 3410, 1547, 1454, and 1033 cm^{-1} after adsorption. In addition, the intensity of peaks was also changed. A similar shifting was also observed in previous report [12]. The outcome reminded that the functional groups of DR/PPy material were involved in the formation of interaction force with dye during adsorption process. In the end, Figure 4 displays the XRD patterns of DR, PPy, and DR/PPy. For the XRD pattern of DR, 16.6° and 22.0° correspond to the diffraction peaks of cellulose. The XRD pattern of PPy has a broaden diffraction peak at 15-30° due to the amorphous feature of PPy. The result was in conformity with the literature [16, 17]. In the XRD pattern of DR/PPy, characteristic diffraction peak of 22.1° related to PPy is integrated with the cellulose peak of DR, which is consistent with the related phenomenon reported in our previous report [1]. This similar phenomenon has been found in other literature [18].

3.2. Analysis of Adsorption Performance of DR/PPy. To illustrate the effectiveness of modification of DR, the comparison in the adsorption efficiency of DR and DR/PPy was conducted, and the result is shown in Figure 5. (The initial pH is the inherent pH of the original dye solution itself, which is very close to 7. So, it was set as 7 for convenience.) It is indicated that the prepared DR/PPy composite was a potential material for the elimination of anionic dyes.

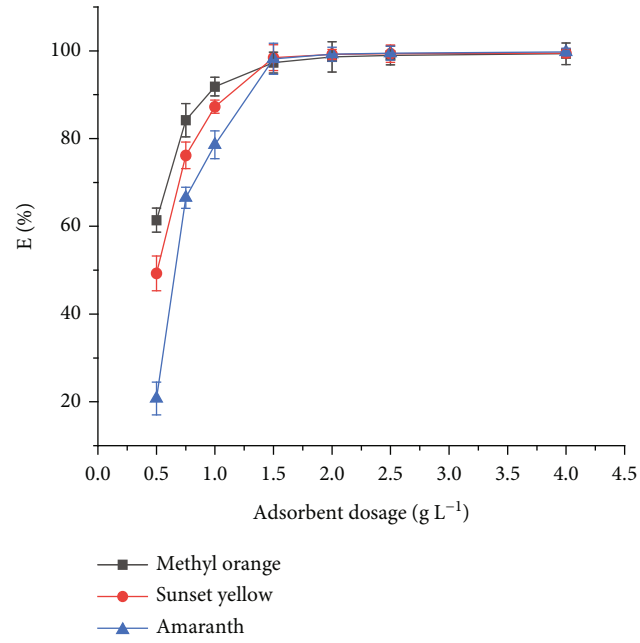

Figure 6: Effect of DR/PPy dosage on the removal performance (conditions: temperature of 40°C, pH of 7, C_0 of 100 μg mL^{-1}, and contacting time of 23 h).

The quantitative effect of DR/PPy for dye elimination was evaluated via varying adsorbent dosage within the range of 0.5-4.0 g L^{-1} with an initial dye concentration of 100 μg mL^{-1}. The result is shown intuitively in Figure 6. It was displayed

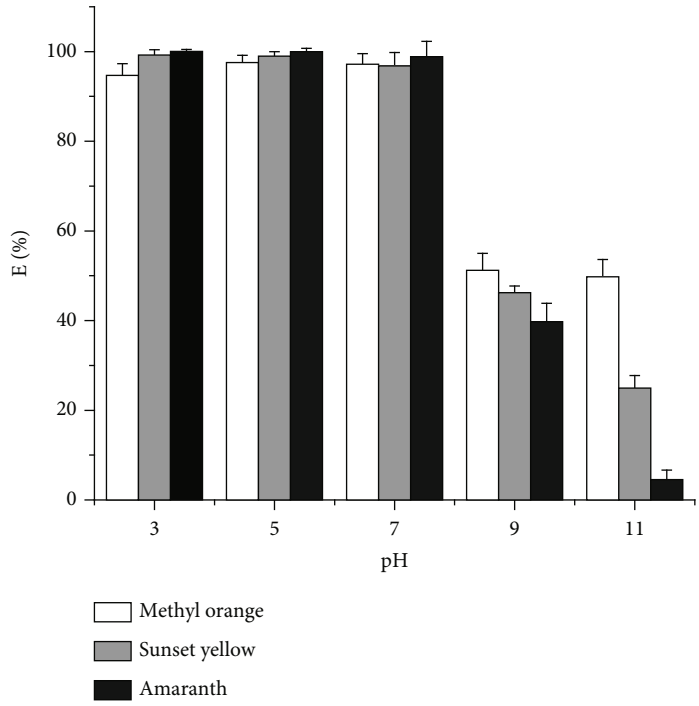

FIGURE 7: Effect of pH on the removal performance (conditions: DR/PPy dosage of 1.5 g L^{-1}, temperature of 40°C, C_0 of 100 μg mL^{-1}, and contacting time of 23 h).

that DR/PPy exhibited increasing removal efficiency of methyl orange from 61.41% to 99.35%, sunset yellow from 49.27% to 99.49%, and amaranth from 20.75% to 99.73%, respectively. The continuous increasing removal efficiency could be ascribed to the larger surface area and greater available active sites at higher adsorbent dosage. Actually, the increasing trend of removal efficiency was not obvious at the amount of adsorbent from 1.5 g L^{-1} to 4.0 g L^{-1}. It is because most of the dyes have been adsorbed onto the DR/PPy at the dosage of 1.5 g L^{-1}. According to the experimental data, the removal efficiencies of DR/PPy for methyl orange, sunset yellow, and amaranth at adsorbent dosage of 1.5 g L^{-1} reached 97.31%, 98.48%, and 98.20%, respectively. Considering the principle of removal efficiency and cost-saving, an appropriate adsorbent dosage of 1.5 g L^{-1} was selected for the subsequent adsorption tests.

The pH of solution could change the surface properties of DR/PPy material and the existing state of studied dye. This will affect the adsorption efficiency [19]. Figure 7 shows the impact of pH value on the adsorptivity of DR/PPy material for each dye under a wide pH range of 3-11. It was observed that higher removal efficiencies were achieved under acidic conditions. At acidic pH, positive surface charge of DR/PPy was produced via its protonated amine group. This could provide enhancing electron affinity with anionic adsorbate via electrostatic attraction (polarization phenomenon). Just right, sulfonate groups of methyl orange, sunset yellow, and amaranth provided the anionic center. The electrostatic force between dye molecules and the surface of DR/PPy became weaker at basic pH, which was not conductive to the removal for the anionic target. These results were in conformity with the current assumption of greater removal efficiency under acidic medium. This outcome was consistent with previous reports [12, 20]. Unexpectedly in methyl orange, the removal efficiency increased from 94.73% to 97.49% within the pH from 3 to 5. It was owing to the fact that methyl orange acquired partial positive charge on the N-atom at lower pH. In this case, the electrostatic attraction between methyl orange and DR/PPy becomes weak. A similar tendency was also discovered for the removal of methyl orange by MChs/PPy [12].

The effects of initial dye concentrations (100, 150, and 200 μg mL^{-1}) and adsorbate/adsorbent interaction time (5-360 min) on the adsorption performance of DR/PPy for removing of methyl orange, sunset yellow, and amaranth are presented in Figure 8. The result clearly revealed that removal efficiency and adsorption capacity increased initially with a fast rate and gradually tended to equilibrium (see Figures 8(a)–8(c)). At the early stage, an abundance of available surface-active adsorption sites was easy approachable for the adsorbate target. But the adsorption rate was gradually reduced with the extension of time, which was due to the occupation of surface-active sites of DR/PPy via adsorbate molecules. Mashkoor and Nasar also believed that the active sites on the surface of MChs/PPy adsorbent play key role in the adsorption behavior [12]. As shown in Figure 8(d), it was visibly found that the adsorption capacity rose with the growing trend of initial dye concentration. Actually, at the early stage in adsorption process, it is clearly seen that the removal degree of methyl orange onto DR/PPy was greater than that of sunset yellow and amaranth, respectively, while with some exceptions. It may be due to the size of dye molecule, which will influence the instantaneous diffusion of dye molecules to the surface of DR/PPy [12]. Subsequently, the kinetics behind the adsorption of the three

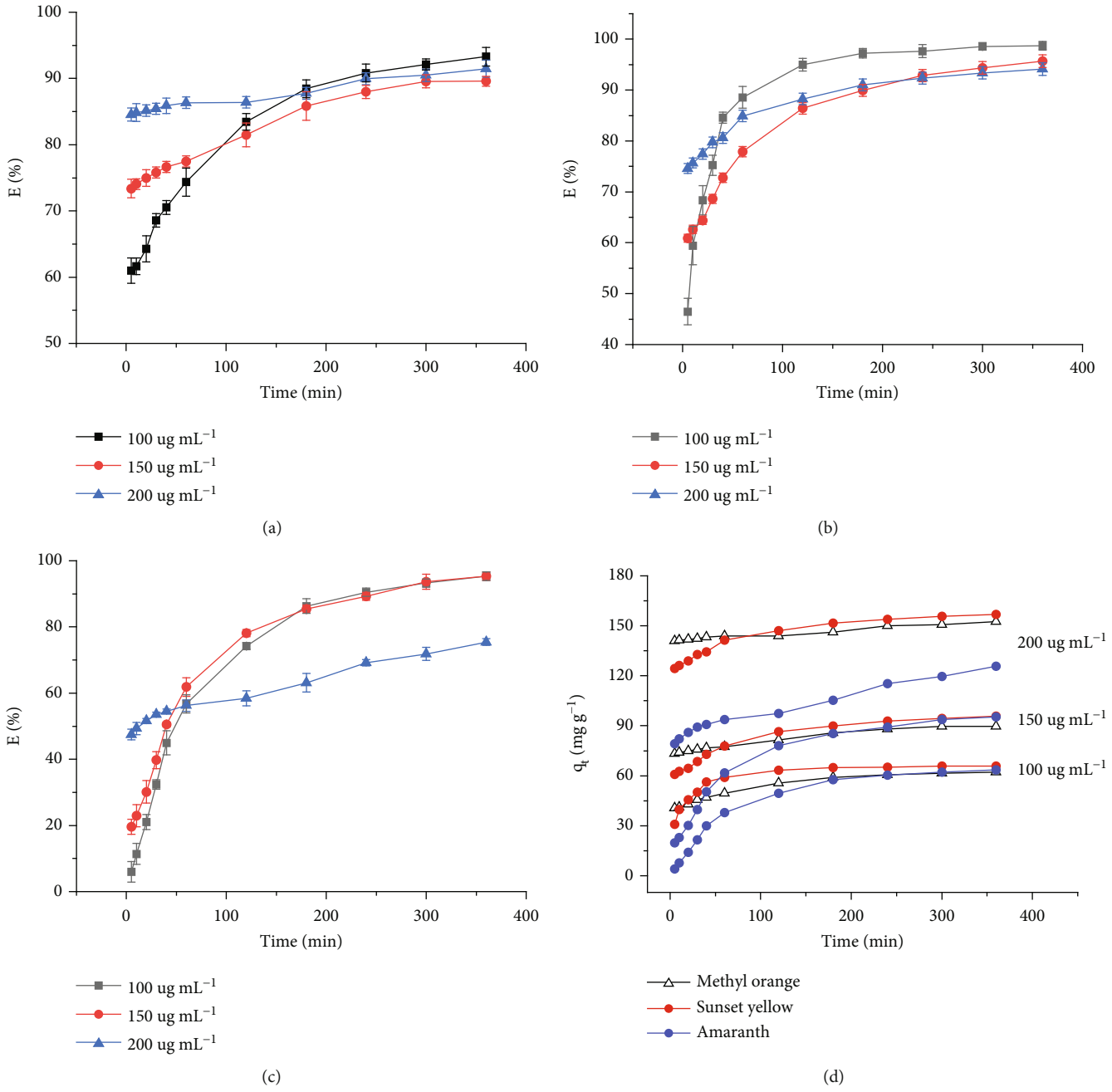

Figure 8: Effects of time and initial dye concentration on the removal performance for (a) methyl orange, (b) sunset yellow, and (c) amaranth, respectively, as well as (d) their corresponding adsorption capacity (conditions: DR/PPy dosage of 1.5 g L^{-1}, pH of 5, and temperature of 40°C).

explored dyes was researched in detail via pseudo-first-order, pseudo-second-order, and intraparticle diffusion kinetic equations. These obtained kinetic parameters for different models are summarized in detail in Table 1, and the most appropriate fitting models are shown in Figures 9(a), 9(c), and 9(e). According to the results, the adsorption towards methyl orange, sunset yellow, and amaranth on DR/PPy conformed to the pseudo-second-order model with higher R^2 values, which were found to be closer to 1. Meanwhile, the calculated values of $q_{e,cal}$ for methyl orange, sunset yellow, and amaranth obtained by the most appropriate fitting model were also closer to the experiment data. Based on the assumption of pseudo-second-order model, chemisorption is the limited step during the adsorption process. In other words, the strong interaction between DR/PPy adsorbent and dyes was existing [14, 15]. However, high R^2 values of pseudo-first-order model could not be ignored, indicating that part of active sites was occupied physically. Hence, the removal of anionic dyes by DR/PPy could be said to be a combination of chemical-physical process. Analogical

Table 1: Kinetic parameters for different models (conditions: DR/PPy dosage of 1.5 g L^{-1}, pH of 5, and temperature of 40°C).

Dye	C_0 (μg mL^{-1})	Pseudo-first-order			Pseudo-second-order			Intraparticle diffusion		
		$q_{e,cal}$	k_1	R^2	$q_{e,cal}$	k_2	R^2	R^2 (step 1)	R^2 (step 2)	R^2 (step 3)
Methyl orange	100	22.86	0.0035	0.9937	63.37	0.0015	0.9988	0.9745	0.9915	0.9830
	150	22.58	0.0017	0.9806	90.42	0.0018	0.9991	0.9963	0.9894	0.9062
	200	17.83	0.0012	0.9663	151.98	0.0025	0.9996	0.9839	0.8062	0.9396
Sunset yellow	100	22.28	0.0059	0.9603	67.34	0.0019	0.9999	0.9653	0.9606	0.9446
	150	35.65	0.0032	0.9872	97.37	0.0010	0.9989	0.9589	0.9744	0.9777
	200	34.70	0.0023	0.9687	157.98	0.0012	0.9997	0.9677	0.9996	0.9941
Amaranth	100	57.24	0.0039	0.9818	77.46	0.0002	0.9968	0.9835	0.9991	0.9887
	150	74.73	0.0042	0.9922	105.49	0.0002	0.9964	0.9715	0.9802	0.9806
	200	76.61	0.0010	0.9869	124.69	0.0006	0.9917	0.9885	0.9240	0.9820

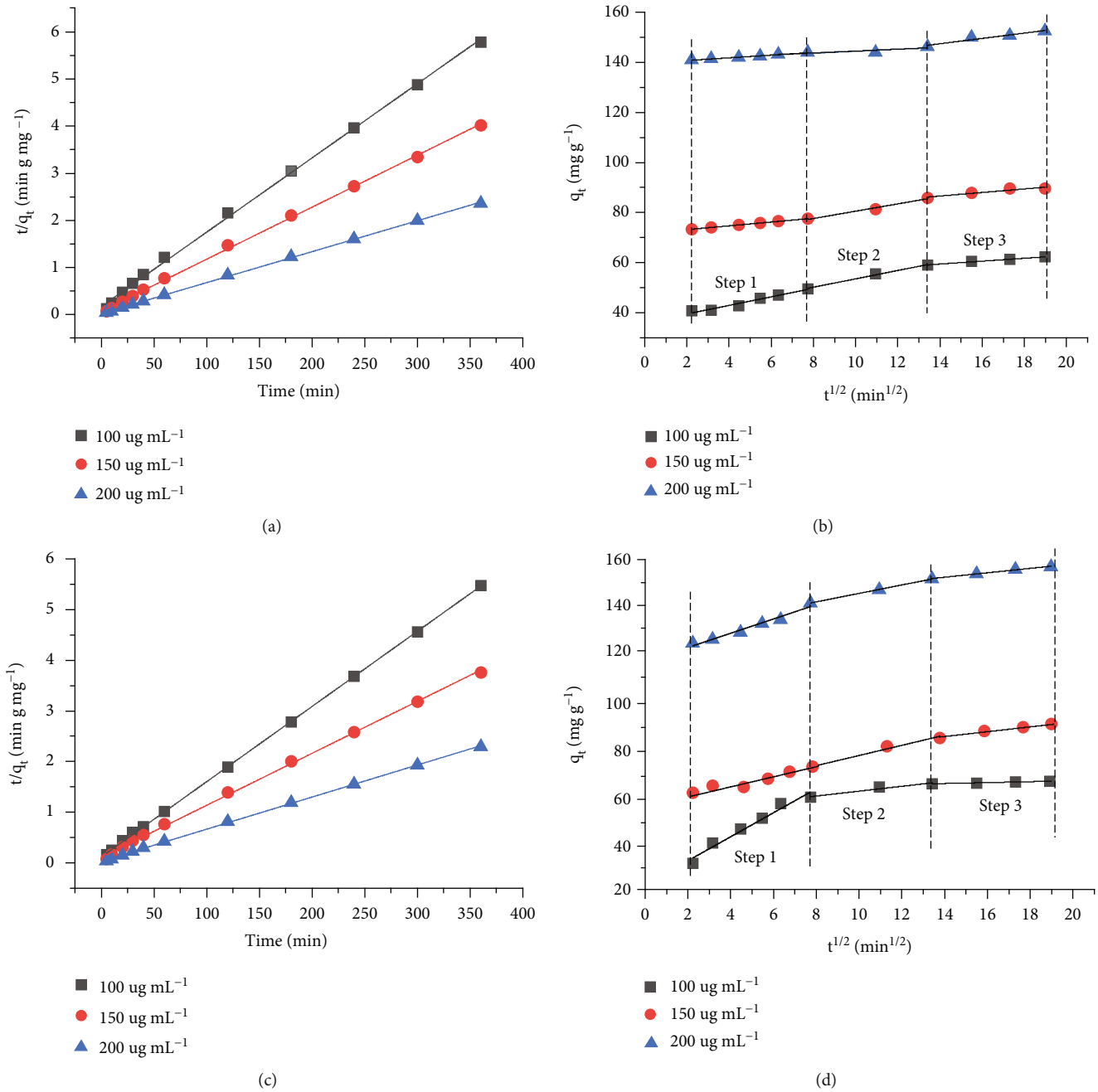

Figure 9: Continued.

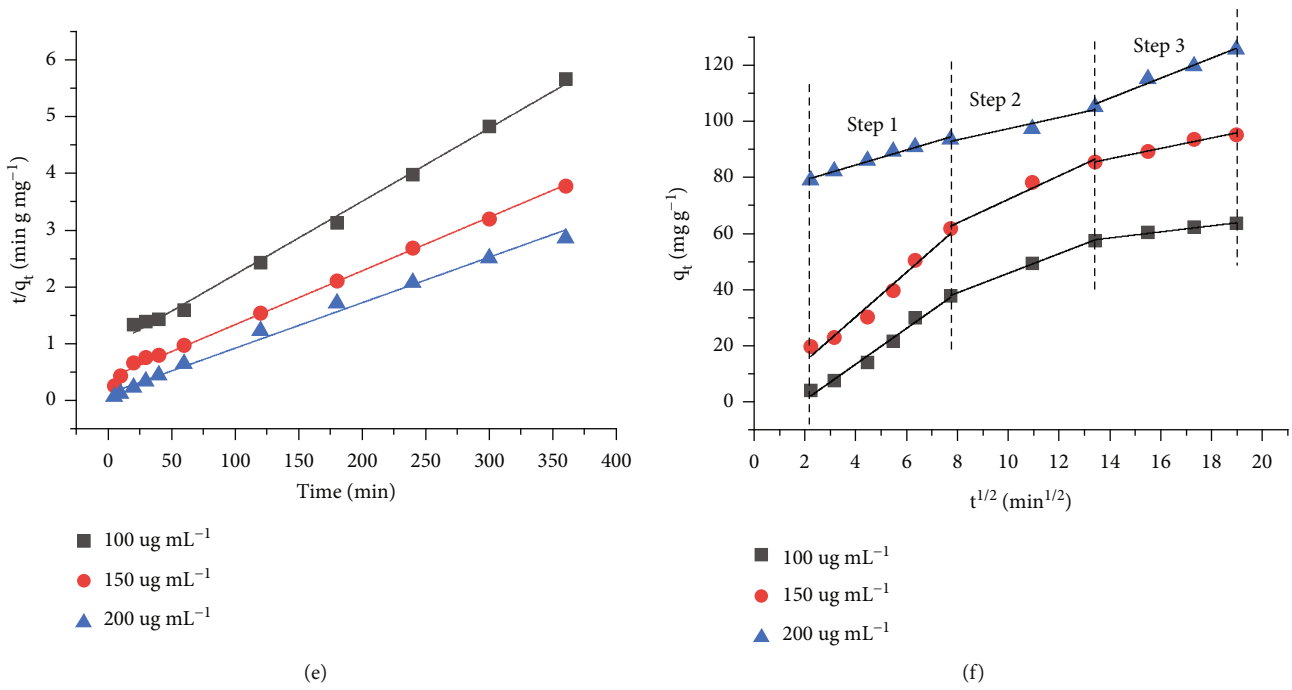

FIGURE 9: Pseudo-second-order model fitted results ((a) methyl orange, (c) sunset yellow, and (e) amaranth) and intraparticle diffusion model fitted results ((b) methyl orange, (d) sunset yellow, and (f) amaranth).

discovery has also been reported by literatures [1, 14]. In addition, intraparticle diffusion model was adopted to excavate the comprehensive mechanism involved in the adsorption of methyl orange, sunset yellow, and amaranth onto DR/PPy. The obtained results are displayed in Figures 9(b), 9(d), and 9(f). It was indicated that the plotting results were not linear over $t^{1/2}$ but making up via three linear steps. At the initial step, instantaneous diffusion of adsorbate molecules (methyl orange, sunset yellow, or amaranth) to the surface of DR/PPy was appeared. Then, the adsorption rate was gradually reduced, which was due to the diffusion resistance. This result was consistent with the related phenomenon reported in previous reference [15].

The adsorption equilibrium data for methyl orange, sunset yellow, and amaranth on the DR/PPy were inspected. Subsequently, the Freundlich and Langmuir isotherm models were adopted to fit the obtained data. The results are given Figure 10 and Table 2. It could be seen that the q_e of DR/PPy rapidly increased and gradually tended to balance with the increase of C_e. In addition, the values of q_e gradually enhanced with increasing temperature. The results demonstrated that the increasing temperature is really conducive to the elimination of each dye, which might be owing to the endothermic feature of the adsorption system. The fitting result indicated that the Langmuir model uncovered greater R^2 values compared with the Freundlich isotherm model. It suggested that the adsorption for methyl orange, sunset yellow, and amaranth uptake was monomolecular layer adsorption [12, 15]. The maximum adsorption capacities of methyl orange, sunset yellow, and amaranth were 193.05, 171.23, and 147.71 mg g^{-1} at 50°C, respectively. This outcome was consistent with the aforementioned conclusion (in the part of pH effect) that electrostatic attraction might be the primary force involved in the adsorption system. Moreover, according to the Langmuir model, a dimensionless quantity RL($R_L = 1/(1 + K_l C_0)$) could be applied to indicate the feasibility of adsorption of dyes onto the DR/PPy. During the initial dye concentrations 50-300 μg mL^{-1}, the values of R_L at 20°C-50°C were obtained to be in the range of 0.0081-0.0746 for methyl orange, 0.0054-0.0586 for sunset yellow, and 0.0012-0.0411 for amaranth, respectively. It is fact that the value of R_L decides whether the adsorption system is linear (1) or irreversible (0), favorable (0-1), or unfavorable (>1). In our study, R_L values at examined initial dye concentrations were all within range of 0 to 1, which manifests the favorable performance of the adsorption for target dyes.

Thermodynamic parameters are critical to reveal the feasibility and characteristic of the adsorption system. Table 3 illustrates the obtained thermodynamic parameters at various temperatures ranging from 288 K to 318 K. All negative values of ΔG within the investigated temperature expressed the spontaneity of adsorption process [15, 21]. The ΔG values in absolute terms enlarged with the rising of temperature. Moreover, the adsorption of methyl orange, sunset yellow, and amaranth onto DR/PPy was endothermic ($\Delta H > 0$). A higher temperature is more conducive to the adsorption. The positive ΔS, indicating the entropy increase of the adsorption process, confirmed increase in randomness and disorder at solid-liquid interface.

3.3. Mixed Adsorption Effect. The mixed adsorption behavior of DR/PPy material was assessed for the ternary mixture of

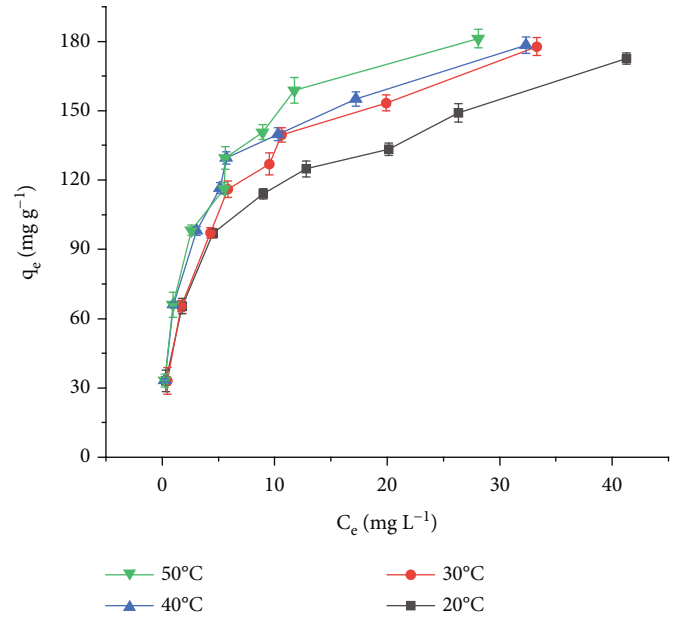

(a)

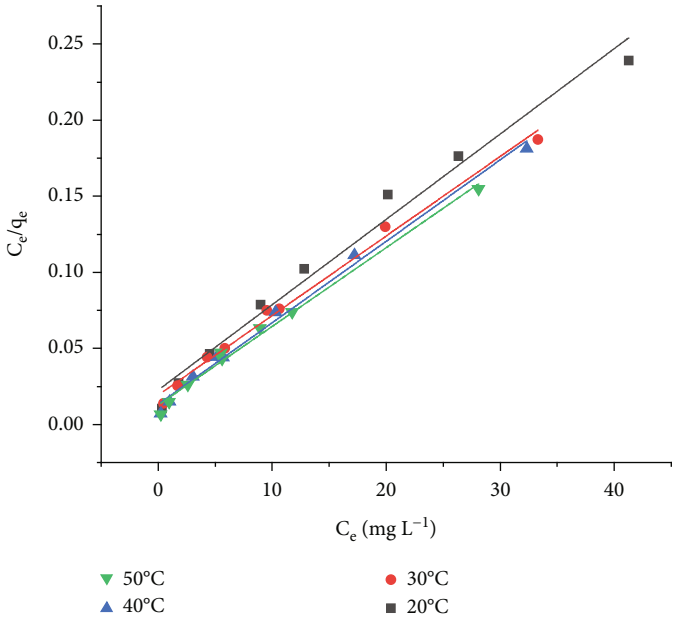

(b)

Figure 10: Continued.

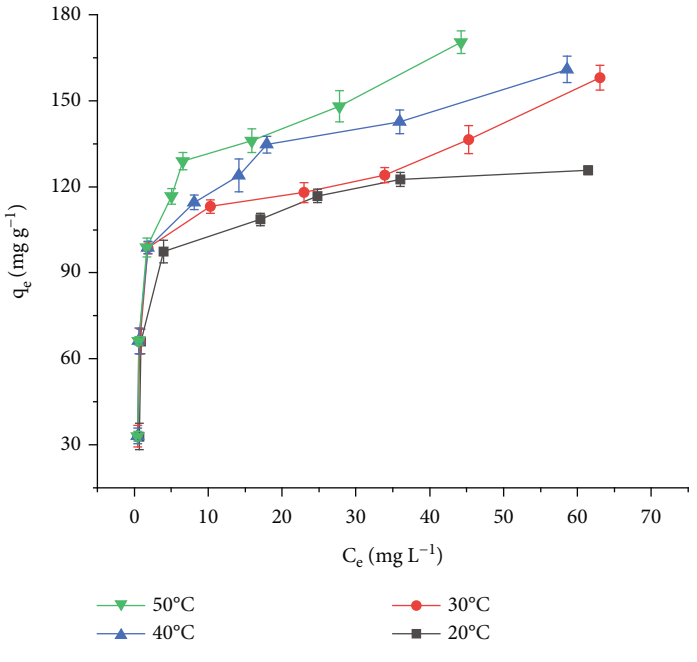

(c)

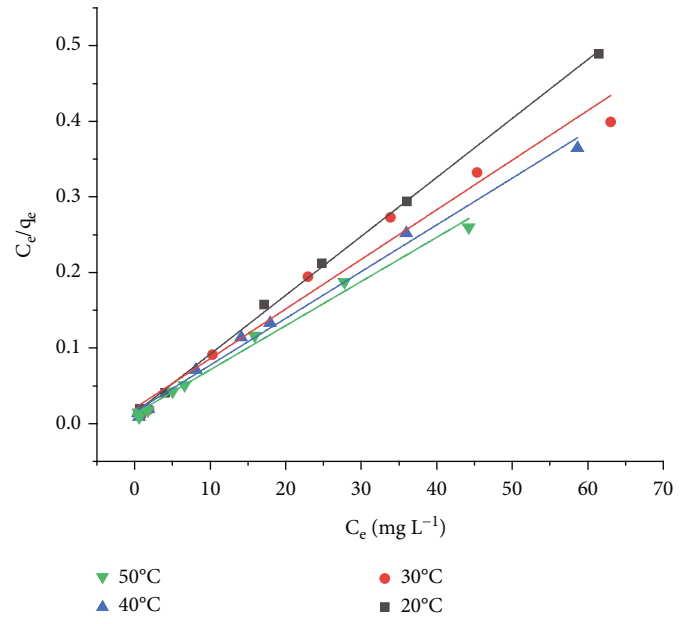

(d)

Figure 10: Continued.

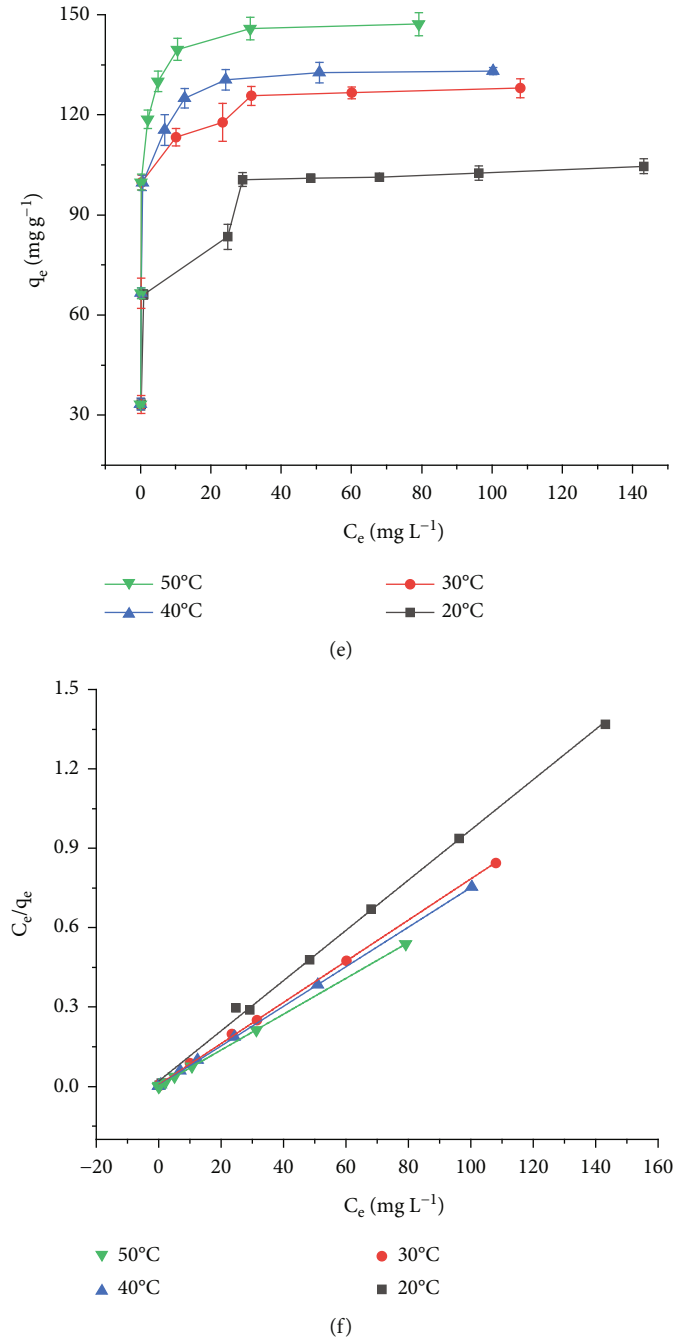

Figure 10: Equilibrium isotherms at different temperatures ((a) methyl orange, (c) sunset yellow, and (e) amaranth) and corresponding Langmuir isotherm plot ((b) methyl orange, (d) sunset yellow, and (f) amaranth).

methyl orange, sunset yellow, and amaranth with different concentrations. The experimental results obtained are illustrated in Table 4. It was observed that the DR/PPy material had a competitive adsorption performance for mixture dyes with respect to removal efficiency. Though the removal efficiencies for mixture dyes were relatively inferior to the initial results with each of the dyes separately, the DR/PPy still exhibited satisfactory adsorption performance for the removal of methyl orange, sunset yellow, and amaranth in ternary mixture. The result showed that DR/PPy material has great potential to eliminate methyl orange, sunset yellow, and amaranth ternary mixture.

3.4. Mechanism. Positive surface charge of adsorbent was produced via the protonated amine group of DR/PPy under acidic medium. Fortunately, methyl orange, sunset yellow, and amaranth are anionic dyes, which have $-SO_3Na$ groups. The dissociation of dye could bring about the formation of $-SO_3^-$. Therefore, two opposite charge groups were existing in the system. Then, the electrostatic attraction between sulfonate

Table 2: Parameters of applied isotherm models for dye on DR/PPy material (condition: DR/PPy dosage of 1.5 g L^{-1}, contacting time of 23 h, and pH of 5).

Dye	Temperature (°C)	Langmuir				Freundlich		
		q_m	K_l	R^2	R_L	$1/n$	K_f	R^2
Methyl orange	20	178.25	0.2482	0.9812	0.0133-0.0746	0.3350	51.8679	0.9825
	30	191.20	0.2710	0.9919	0.0122-0.0687	0.3916	51.2928	0.9675
	40	186.92	0.4035	0.9930	0.0082-0.0472	0.3416	62.3541	0.9654
	50	193.05	0.4092	0.9914	0.0081-0.0466	0.3575	63.7736	0.9749
Sunset yellow	20	128.21	0.3216	0.9988	0.0103-0.0585	0.2381	53.6526	0.7913
	30	152.44	0.3225	0.9899	0.0077-0.0584	0.2347	59.4889	0.8012
	40	161.81	0.3985	0.9931	0.0062-0.0478	0.2550	62.5046	0.8237
	50	171.23	0.4595	0.9917	0.0054-0.0417	0.2845	64.5022	0.8046
Amaranth	20	105.37	0.4661	0.9984	0.0071-0.0411	0.1557	52.9713	0.8836
	30	128.53	1.2214	0.9997	0.0027-0.0161	0.1466	72.7348	0.6463
	40	133.69	2.0952	0.9999	0.0016-0.0095	0.1540	78.7942	0.8508
	50	147.71	2.8326	0.9999	0.0012-0.0070	0.1304	97.4666	0.9373

Table 3: Thermodynamic values for methyl orange, sunset yellow, and amaranth adsorption (condition: DR/PPy dosage of 1.5 g L^{-1}, C_0 of 200 μg mL^{-1}, contacting time of 23 h, and pH of 5).

Dye	Temperature (K)	ΔG (kJ mol^{-1})	ΔH (kJ mol^{-1})	ΔS (kJ mol^{-1} K^{-1})
Methyl orange	288	-5.5507	24.6863	0.1034
	298	-6.5289		
	308	-8.1226		
	318	-8.4386		
Sunset yellow	288	-3.7738	37.3847	0.1389
	298	-4.1244		
	308	-5.6487		
	318	-7.9800		
Amaranth	288	-1.7943	64.7810	0.2270
	298	-4.0721		
	308	-5.9865		
	318	-8.7444		

Table 4: Mixed adsorption efficiency (condition: DR/PPy dosage of 1.5 g L^{-1}, temperature of 50°C, contacting time of 23 h, and pH of 5).

Number	DR/PPy dosage (g L^{-1})	C_0 (μg mL^{-1})	Removal efficiency (%)		
			Methyl orange	Sunset yellow	Amaranth
1	1.5	100	98.87	97.14	98.34
2	1.5	150	97.73	95.75	95.82
3	1.5	200	92.94	88.90	89.60

groups of methyl orange, sunset yellow, and amaranth and protonated amine groups of DR/PPy becomes functioning [12, 20]. Additionally, other interactions such as π-π and hydrogen-bonding interaction force could also play important roles in the adsorption process [12]. Taking methyl orange as an example, a schematic illustration of plausible mechanism for adsorption of anionic dye onto DR/PPy is given in Figure 11.

3.5. Comparison with Other Materials. The adsorptivity of DR/PPy for methyl orange, sunset yellow, and amaranth was compared with other adsorbents to evaluate its applicability. The compared outcome is illustrated in Table 5. It was observed that DR/PPy was superior to most of adsorbents, such as MChs/PPy [12], zirconium-immobilized bentonite [22], imprinted polymer NPs [23], MWCNTs-PATMSPEDA-Pd-NPs [24], sisal/polypyrrole/polyaniline [14], PPy/starch [25],

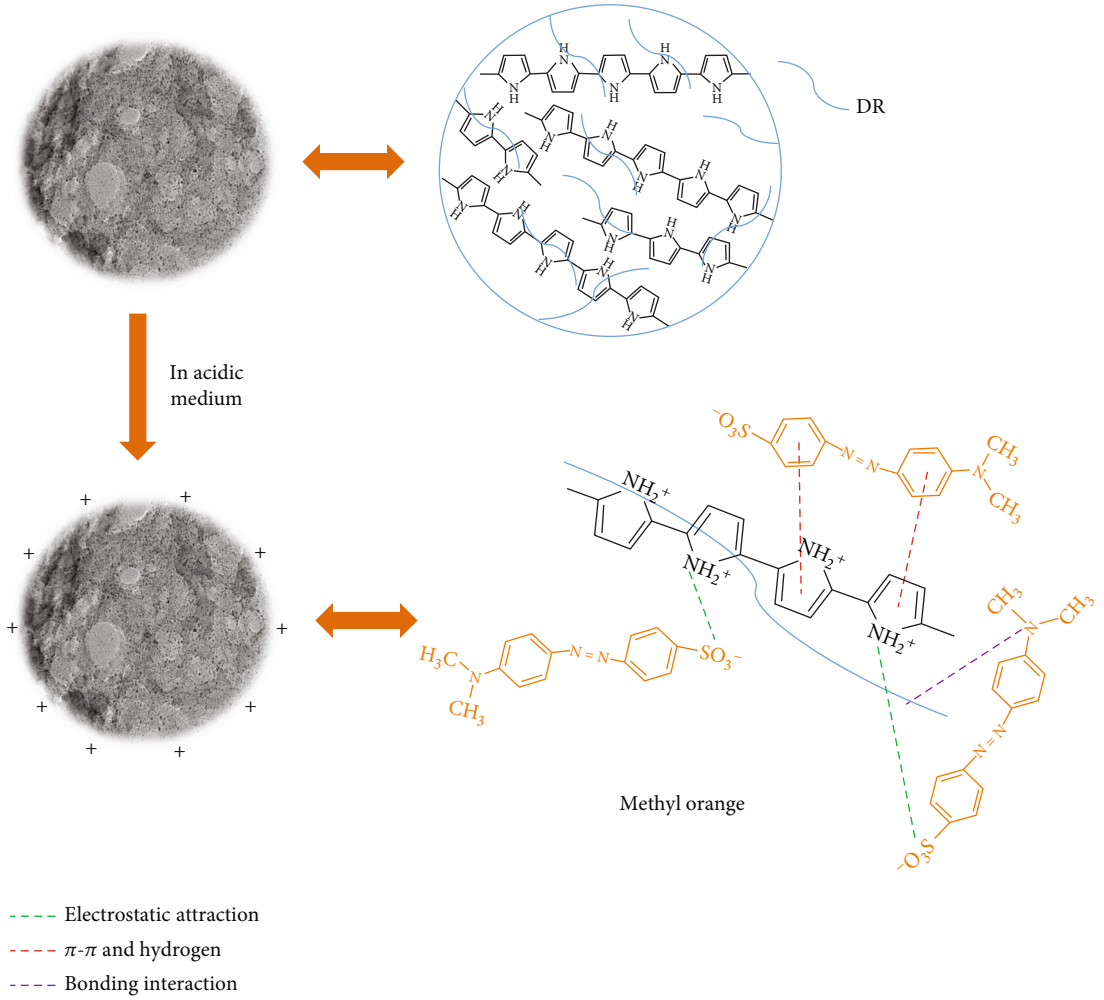

Figure 11: Schematic illustration of plausible mechanism for adsorption of anionic dye onto DR/PPy.

Table 5: Comparison of DR/PPy towards the removal of dye with other adsorbents.

Number	Adsorbents	Dyes	q (mg g^{-1})	Ref.
1	MChs/PPy	Methyl orange/cationic crystal violet	89.29/62.89	[12]
2	Zirconium-immobilized bentonite	Methyl orange	44.13	[22]
3	Amine polymer-modified Fe_3O_4	Amaranth	226.40	[27]
4	PPy/mw nanocomposite	Sunset yellow/Congo red	212.10/147.00	[28]
5	Imprinted polymer NPs	Sunset yellow	144.60	[23]
6	MWCNTs-PATMSPEDA-Pd-NPs	Sunset yellow/erythrosine	59.17/38.76	[24]
7	Activated carbon	Direct green 6	112.35	[26]
8	Aminated avocado	Acid yellow 17/amaranth	42.70/89.20	[29]
9	Sisal/polypyrrole/polyaniline	Reactive orange 5	12.43	[14]
10	PMMA/(rice husk ash)/polypyrrole	Tartrazine/indigo carmine	165.70/142.90	[30]
11	PPy/starch	Acid black dye	66.60	[25]
12	DR/PPy	Methyl orange/sunset yellow/amaranth	193.05/171.23/147.71	This work

and activated carbon [26]. Compared with the above adsorbents, DR/PPy occupies place in the field of adsorption for dyes.

4. Conclusion

The present study indicated that the DR/PPy composite was a desirable adsorbent for the efficient elimination of anionic dyes from aqueous medium. It is the first time that DR/PPy composite was prepared and applied for elimination of dyes. Herein, polypyrrole was introduced into durian rind by in situ polymerization technology to prepare DR/PPy composite, which was confirmed via TEM, SEM, IRS, and XRD in detail. Process variables involving the dosage of DR/PPy, initial dye concentration, pH, adsorption temperature, and contacting time had obvious influences on the performance for the removal of dyes. Under initial concentration of $100\,\mu g\,mL^{-1}$, pH of 7, and DR/PPy dosage of $1.5\,g\,L^{-1}$, the removal efficiency reached 97.31%, 98.48%, and 98.20% for methyl orange, sunset yellow, and amaranth, respectively. The time-dependent adsorption kinetic data of anionic dyes on DR/PPy conformed to the pseudo-second-order kinetic model. Meanwhile, the result fitted by intraparticle diffusion model indicated that the process of methyl orange, sunset yellow, and amaranth molecules onto DR/PPy materials exhibited multiple diffusion steps. The Langmuir model was the most appropriate model for fitting the experimental data. The $q_{m,\max}$ was 193.05, 171.23, and $147.71\,mg\,g^{-1}$ for methyl orange, sunset yellow, and amaranth, respectively. The outcomes of thermodynamic parameter analysis exhibited that the adsorption process of methyl orange, sunset yellow, and amaranth molecules onto DR/PPy was spontaneous and endothermic. In addition, this DR/PPy material showed a satisfactory efficiency for methyl orange, sunset yellow, and amaranth ternary mixture in simultaneous removal. The main mechanism involved in the adsorption system was electrostatic attraction. It was concluded that the route for preparation of DR/PPy was simple and low cost. This work implied the feasibility of preparation DR/PPy composite with durian rind waste to eliminate anionic dyes from wastewater. Excellent removal efficiency, cost-effectiveness, and availability are the chief advantage of DR/PPy. Also, the result provided an attractive alternative for the exploitation and utilization of durian rind biomass for generating new biocomposite to treat similar pollutants.

Data Availability

All relevant data are within the paper.

Conflicts of Interest

The authors declare that they have no conflicts of interest.

Acknowledgments

We really appreciated the support from the University Natural Science Research Project of Anhui Province (no. KJ2021A0884) to undertake this study. This work was supported by the National College Student Innovation Training Program (no. S202210879287).

References

[1] Y. Wang, R. Chen, Z. Dai, Q. Yu, Y. Miao, and R. Xu, "Facile preparation of a polypyrrole modified Chinese yam peel-based adsorbent: characterization, performance, and application in removal of Congo red dye," *RSC Advances*, vol. 12, no. 15, pp. 9424–9434, 2022.

[2] W. Li, B. Mu, and Y. Yang, "Feasibility of industrial-scale treatment of dye wastewater via bio-adsorption technology," *Bioresource Technology*, vol. 277, pp. 157–170, 2019.

[3] U. Kamran, H. N. Bhatti, S. Noreen, M. A. Tahir, and S. J. Park, "Chemically modified sugarcane bagasse-based biocomposites for efficient removal of acid red 1 dye: kinetics, isotherms, thermodynamics, and desorption studies," *Chemosphere*, vol. 291, Part 2, article 132796, 2022.

[4] D. A. González-Casamachin, J. R. De la Rosa, C. J. Lucio-Ortiz et al., "Visible-light photocatalytic degradation of acid violet 7 dye in a continuous annular reactor using ZnO/PPy photocatalyst: synthesis, characterization, mass transfer effect evaluation and kinetic analysis," *Chemical Engineering Journal*, vol. 373, pp. 325–337, 2019.

[5] H. Ma, J. B. Li, W. W. Liu, M. Miao, B. J. Cheng, and S. W. Zhu, "Novel synthesis of a versatile magnetic adsorbent derived from corncob for dye removal," *Bioresource Technology*, vol. 190, pp. 13–20, 2015.

[6] V. Arumugam, P. Sriram, T. J. Yen, G. G. Redhi, and R. M. Gengan, "Nano-material as an excellent catalyst for reducing a series of nitroanilines and dyes: triphosphonated ionic liquid- $CuFe_2O_4$-modified boron nitride," *Applied Catalysis B: Environmental*, vol. 222, pp. 99–114, 2018.

[7] B. H. Hameed and H. Hakimi, "Utilization of durian (*Durio zibethinus* Murray) peel as low cost sorbent for the removal of acid dye from aqueous solutions," *Biochemical Engineering Journal*, vol. 39, no. 2, pp. 338–343, 2008.

[8] H. Sudrajat, A. Susanti, D. K. Y. Putri, and S. Hartuti, "Mechanistic insights into the adsorption of methylene blue by particulate durian peel waste in water," *Water Science and Technology*, vol. 84, no. 7, pp. 1774–1792, 2021.

[9] N. T. Thuong, N. T. T. Nhi, V. T. C. Nhung et al., "A fixed-bed column study for removal of organic dyes from aqueous solution by pre-treated durian peel waste," *Indonesian Journal of Chemistry*, vol. 19, no. 2, pp. 486–494, 2019.

[10] E. Kusrini, A. Usman, F. A. Sani, L. D. Wilson, and M. A. A. Abdullah, "Simultaneous adsorption of lanthanum and yttrium from aqueous solution by durian rind biosorbent," *Environmental Monitoring and Assessment*, vol. 191, no. 8, p. 488, 2019.

[11] M. A. Asbollah, A. H. Mahadi, E. Kusrini, and A. Usman, "Synergistic effect in concurrent removal of toxic methylene blue and acid red-1 dyes from aqueous solution by durian rind: kinetics, isotherm, thermodynamics, and mechanism," *International Journal of Phytoremediation*, vol. 23, no. 13, pp. 1432–1443, 2021.

[12] F. Mashkoor and A. Nasar, "Facile synthesis of polypyrrole decorated chitosan-based magsorbent: characterizations, performance, and applications in removing cationic and anionic dyes from aqueous medium," *International Journal of Biological Macromolecules*, vol. 161, pp. 88–100, 2020.

[13] T. Shahnaz, S. M. M. Fazil, V. C. Padmanaban, and S. Narayanasamy, "Surface modification of nanocellulose using polypyrrole for the adsorptive removal of Congo red dye and chromium in binary mixture," *International Journal of Biological Macromolecules*, vol. 151, pp. 322–332, 2020.

[14] A. Khadir, M. Negarestani, and H. Ghiasinejad, "Low-cost sisal fibers/polypyrrole/polyaniline biosorbent for sequestration of reactive orange 5 from aqueous solutions," *Journal of Environmental Chemical Engineering*, vol. 8, no. 4, article 103956, 2020.

[15] M. Tanzifi, M. T. Yaraki, Z. Beiramzadeh et al., "Carboxymethyl cellulose improved adsorption capacity of polypyrrole/CMC composite nanoparticles for removal of reactive dyes: experimental optimization and DFT calculation," *Chemosphere*, vol. 255, article 127052, 2020.

[16] Y. Deng, X. Zhao, J. Luo, Z. Wang, and J. Tang, "Magnetic recyclable $CoFe_2O_4$@PPy prepared byin situFenton oxidization polymerization with advanced photo-Fenton performance," *RSC Advances*, vol. 10, no. 4, pp. 1858–1869, 2020.

[17] X.-r. Pan, M. Wang, X.-d. Qi et al., "Fabrication of sandwich-structured PPy/MoS_2/PPy nanosheets for polymer composites with high dielectric constant, low loss and high breakdown strength," *Composites Part A Applied Science and Manufacturing*, vol. 137, article 106032, 2020.

[18] S. Rafiaee, M. R. Samani, and D. Toghraie, "Removal of hexavalent chromium from aqueous media using pomegranate peels modified by polymeric coatings: effects of various composite synthesis parameters," *Synthetic Metals*, vol. 265, article 116416, 2020.

[19] Z. Chen and K. Pan, "Enhanced removal of Cr(VI) via in-situ synergistic reduction and fixation by polypyrrole/sugarcane bagasse composites," *Chemosphere*, vol. 272, article 129606, 2021.

[20] G. Derouich, S. A. Younssi, J. Bennazha, J. A. Cody, M. Ouammou, and M. El Rhazi, "Development of low-cost polypyrrole/sintered pozzolan ultrafiltration membrane and its highly efficient performance for Congo red dye removal," *Journal of Environmental Chemical Engineering*, vol. 8, no. 3, article 103809, 2020.

[21] V. Priyan, N. Kumar, H. K. Rajendran, J. Ray, and S. Narayanasamy, "Sequestration and toxicological assessment of emerging contaminants with polypyrrole modified carboxymethyl cellulose (CMC/PPY): case of ibuprofen pharmaceutical drug," *International Journal of Biological Macromolecules*, vol. 221, pp. 547–557, 2022.

[22] R. Huang, C. Hu, B. Yang, and J. Zhao, "Zirconium-immobilized bentonite for the removal of methyl orange (MO) from aqueous solutions," *Desalination and Water Treatment*, vol. 57, no. 23, pp. 10646–10654, 2016.

[23] G. Yang, H. Huang, J. Chen et al., "Preparation of ionic liquids functionalized nanodiamonds-based composites through the Michael addition reaction for efficient removal of environmental pollutants," *Journal of Molecular Liquids*, vol. 296, article 111874, 2019.

[24] R. Karimi, F. Yousefi, M. Ghaedi, K. Dashtian, and M. Montazerozohori, "Efficient adsorption of erythrosine and sunset yellow onto modified palladium nanoparticles with a 2-diamine compound: application of multivariate technique," *Journal of Industrial and Engineering Chemistry*, vol. 48, pp. 43–55, 2017.

[25] S. Noreen, H. N. Bhatti, M. Iqbal, F. Hussain, and F. M. Sarim, "Chitosan, starch, polyaniline and polypyrrole biocomposite with sugarcane bagasse for the efficient removal of acid black dye," *International Journal of Biological Macromolecules*, vol. 147, pp. 439–452, 2020.

[26] A. Geetha and N. Palanisamy, "Studies on adsorptive removal of direct green 6 using a non-conventional activated carbon and polypyrrole composite," *Desalination and Water Treatment*, vol. 57, no. 43, pp. 20534–20543, 2016.

[27] Y. Huo, H. Wu, Z. Wang et al., "Preparation of core/shell nanocomposite adsorbents based on amine polymer-modified magnetic materials for the efficient adsorption of anionic dyes," *Colloids and Surfaces A: Physicochemical and Engineering Aspects*, vol. 549, pp. 174–183, 2018.

[28] R. S. Aliabadi and N. O. Mahmoodi, "Synthesis and characterization of polypyrrole, polyaniline nanoparticles and their nanocomposite for removal of azo dyes; sunset yellow and Congo red," *Journal of Cleaner Production*, vol. 179, pp. 235–245, 2018.

[29] V. S. Munagapati, H. Y. Wen, Y. Vijaya et al., "Removal of anionic (acid yellow 17 and amaranth) dyes using aminated avocado (*Persea americana*) seed powder: adsorption/desorption, kinetics, isotherms, thermodynamics, and recycling studies," *International Journal of Phytoremediation*, vol. 23, no. 9, pp. 911–923, 2021.

[30] H. D. da Rocha, E. S. Reis, G. P. Ratkovski et al., "Use of PMMA/(rice husk ash)/polypyrrole membranes for the removal of dyes and heavy metal ions," *Journal of the Taiwan Institute of Chemical Engineers*, vol. 110, pp. 8–20, 2020.